JOURNAL OF AIRCRAFT
Vol. 45, No. 6, November–December 2008

# Effect of Humidity on Transonic Flow

J. C. Huang* and R. I. Gault†
*Queen's University of Belfast,*
*BT9 5AH Belfast, Ireland, United Kingdom*
E. Benard‡
*University of Glasgow,*
*G12 8QQ Glasgow, Scotland, United Kingdom*
and
S. Raghunathan§
*Queen's University of Belfast,*
*BT9 5AH Belfast, Ireland, United Kingdom*

DOI: 10.2514/1.37464

**An experimental investigation of the effects of humidity-induced condensation on shock/boundary-layer interaction has been conducted in a transonic wind-tunnel test. The test geometry considered was a wall-mounted bump model inserted in the test section of the wind tunnel. The formation of a λ-shape condensation shock wave was shown from schlieren visualization and resulted in a forward movement of the shock wave, reduced shock wave strength, and reduced separation. Empirical correlations of the shock wave strength and humidity/dew point temperature were established. For humidity levels below 0.15 or a dew point temperature of 268 K, the effect of humidity was negligible. The unsteady pressure measurements showed that if a condensation shock wave formed and interacted with a main shock wave, the flow becomes unsteady with periodic flow oscillations occurring at 720 Hz.**

## Nomenclature

| | | |
|---|---|---|
| $C$ | = | bump chord length |
| $H$ | = | shape factor |
| $L$ | = | separation length |
| $M$ | = | isentropic Mach number |
| $M^*$ | = | $M/M_{\text{dry}}$ |
| $P$ | = | static pressure |
| $P_{\text{rms}}/q^*$ | = | $P_{\text{rms}}/q/(P_{\text{rms}}/q)_{\text{dry}}$ |
| $P_{\text{rms}}$ | = | rms fluctuating pressure |
| $q$ | = | freestream dynamic pressure |
| $Re_\theta$ | = | Reynolds number based on the momentum thickness |
| $RH$ | = | stagnation relative humidity level at the inlet of test section |
| $T$ | = | stagnation temperature |
| $Tu$ | = | turbulence level |
| $T_d$ | = | stagnation dew point temperature |
| $X$ | = | streamwise distance |
| $X^*$ | = | dimensionless parameter |
| $\gamma(T, RH)$ | = | function of temperature and humidity |
| $\delta$ | = | boundary-layer thickness |
| $\Delta Xs^*$ | = | forward shock wave shift $= (Xs - Xs_{\text{dry}})/Xs_{\max}$ |
| $\Delta P_s^*$ | = | pressure rise of separation |

*Subscripts*

| | | |
|---|---|---|
| dry | = | air dry condition at $T_d = 262$ K or $RH = 0.10$ |
| $s$ | = | peak |
| $W$ | = | upstream of shock wave |
| $\infty$ | = | freestream |

Presented as Paper 358 at the 46th AIAA Aerospace Sciences Meeting and Exhibit, Reno, NV, 7–10 January 2008; received 10 March 2008; accepted for publication 17 June 2008. 

*Research Fellow, Center of Excellence for Integrated Aircraft Technology, School of Mechanical and Aeronautical Engineering. Member AIAA.

†Research Fellow, Center of Excellence for Integrated Aircraft Technology, School of Mechanical and Aeronautical Engineering. Member AIAA.

‡Senior Lecturer, Department of Aerospace Engineering. Member AIAA.

§Bombardier-Royal Academy Chair, Center of Excellence for Integrated Aircraft Technology, School of Mechanical and Aeronautical Engineering. Associate Fellow AIAA.

## I. Introduction

CONDENSATION is likely to occur on a surface, in transonic flight under humid conditions, having an influence on the aerodynamic performance, such as lift and drag [1–3]. Humidity-induced condensation needs to be taken into account in understanding the aerodynamic performance of aircraft.

As a moist flow accelerates over the upper surface of an aerofoil, the local pressure and temperature decreases and, if the saturation condition is reached, condensation of the water vapor occurs and liquid droplets nucleate [3,4]. The condensation process releases heat to the surrounding gas, leading to thermodynamic changes of the gas properties. Often, condensation develops in a nonequilibrium process during transonic wind-tunnel tests, where rapid expansions of highly purified vapors in supersonic nozzles or over aerofoils can be present [4]. In the homogeneous condensation process, spontaneous fluctuations in the water vapor initiate a nucleation of water droplets, and a condensation compression wave can be observed under certain conditions [5]. The condensation process, more often than not, can be observed in an in-draft transonic wind tunnel operating under atmospheric conditions [4].

Recent studies on condensation process effects on shock waves were conducted by Schnerr and Dohrmann [1,2], Rusak and Lee [4], and Doerffer et al. [6,7]. From their experiments, they observed that significant differences in the normal shock wave structure and shock-induced separation were sensitive to relative humidity variations. For transonic flow over an aerofoil, increases in humidity levels lead to the appearance of condensation. This nonadiabatic phenomenon causes heat addition, retarding the flow, and, because of the condensation, the Mach number of the flow is reduced, which leads to a weakening of the shock wave strength. Hence, the disturbances to the boundary layer become smaller and separation may disappear [6,7].

Humidity effects on the shock wave position were examined by Schnerr and Dohrmann [1,2], who used an inviscid fluid flow model for their predictions. A forward shock wave shift was found up until the relative humidity level reached 0.50. This shift was associated with heat addition, controlled by the flow condensation process. The same experimental conclusion on shock wave shift was publicized by Evans [8]. Nevertheless, the heat addition caused by condensation affects the pressure distribution along the surface of an aerofoil. Depending on the aerofoil geometry and different heat supply conditions, the pressure drag achieved can be half of the classic dry air case at the same Mach number.

In transonic flow where the shock wave appears, the condensation changes the structure of the entire supersonic flow region around the aerofoil and a double-shock system may appear [1,2]. As a result, moist air around an aerofoil is likely to create complicated flowfields, which are different from dry air, and cause dramatic changes in aerodynamic performance.

Studies on a nonequilibrium condensation in a Laval nozzle have been carried out by Matsuo et al. [9,10], showing that, when the heat addition exceeded a certain limit, the flow became unstable with self-excited periodic oscillations and complex dynamics. Similar conclusions were found in supersonic flows [11]. Rusak and Lee [4] used an inviscid small-disturbance computational fluid dynamics (CFD) model on homogeneous condensation over an aerofoil. They concluded that there were many difficulties in finding a steady-state solution in high-humidity levels. Therefore, in an environment where the humidity is high, the flow becomes unsteady and mechanisms of stability loss become an important issue.

Transonic shock wave boundary-layer interaction over a wall-mounted bump has been used as a benchmark for CFD validations, owing to the fact that it characterizes complicated physical phenomena. In many transonic flow experiments, the humidity is controlled, but the effect in wind-tunnel tests is not often quantified. Indeed, the underlying humidity effect on shock/boundary-layer interaction in a transonic flow is still not fully understood. In the present study, an experimental program was undertaken to quantify the effect of humidity on transonic flow. In particular, the effects on shock wave strength and position were examined, along with the interaction between the main shock wave and the condensation shock wave. Steady and unsteady pressure measurements were measured out in conjunction with schlieren visualization. Correlations between shock wave strength and position were established and compared with other available experimental and numerical data for transonic flows.

## II. Experimental Program

Experiments were conducted in an in-draft transonic wind tunnel at Queen's University Belfast [12,13]. The air storage balloon is connected to a vacuum tank via a settling chamber, test section, and diffuser. Two silica air dryers were placed before the inlet to the balloon to vary the humidity levels. The test section dimensions are $101.6 \times 101.6 \times 979$ mm for the height, width, and length, respectively, illustrated in Fig. 1. A contoured wall was implemented in the roof of the test section, opposite the bump. The purpose of using a contoured wall was to eliminate the pressure gradient effect on the shock wave boundary-layer interaction and to mimic a free-flight condition. The wall-mounted bump has a maximum height of 9.14 mm and chord length of 101.6 mm, as shown in Fig. 1. The geometry of the bump has been tested extensively and the leading edge is located 549.2 mm from the inlet of the test section. The reference point was taken at the bump leading edge.

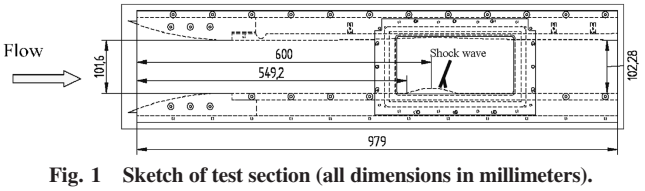


**Fig. 1 Sketch of test section (all dimensions in millimeters).**

Flow visualization and steady flow measurements were initially taken to understand the basic flow parameters, such as shock wave position and separation length. *Z*-type schlieren and china clay flow visualization provided a means to identify the onset of the shock wave and separation regions. The schlieren images were recorded using a high-speed camera (FASTCAM-X 128PCI 4K) with a frequency of 1000 fps and exposure time of 0.001 s. Wall static pressures were measured from the centerline of the bump model and recorded using a pressure scanner (PSI ESP 32HD) with 10 Hz frequency for 32 individual ports.

Piezoresistive sensors (Kulite XCS-062-10D) were used for the unsteady pressure measurements. The sensors were connected to an interface board (manufactured by AA-Lab Gage-3000) and were supplied with 10 V. A built-in amplifier was employed to improve the signal-to-noise ratio together with a 20 kHz low-pass filter. Three piezoresistive pressure sensors were installed in a 2.4-mm-wide cavity through the base of the model, leading to 0.5-mm-diam orifices on the surface. The natural frequency of the cavity was estimated to be 10 kHz. All the sensors were sealed using a silicon rubber. Unsteady measurements were recorded at a sampling frequency of 50 kHz through a National Instruments PCI-6143 card, which allows simultaneous three-channel data acquisition.

From the flow visualization, the shock wave location was identified at $X^* = 0.63$, where $X^*$ is a dimensionless distance related to the bump chord length. The pressure sensors were then installed before, adjacent, and after this shock wave location ($X^* = 0.60$, 0.63, 0.66). Each test lasted 10 s, during which data were recorded over an 8 s window. Error bars for the pressure measurements uncertainties are shown in the results. These are mainly due to the accuracy of the transducers.

During the experiments, the silica dryers were used to control the humidity level of the air before entering the test section. A humidity sensor was installed in the settling chamber, measuring humidity levels ranging from 0.1 to 0.55. Typically, the relative humidity level at the test section inlet was found to decrease from 0.08 to 0.04 during a series of tests. During each test, the humidity and temperature levels were recorded from sensors in the settling chamber. Relevant aerodynamic parameters are listed in Table 1. The tunnel freestream Mach number was controlled through back choke and values ranging from $M_\infty = 0.780$ to 0.805 were used for the tests. The measured inlet temperature and pressure were, in general, at $292 \pm 2$ K and $1.013 \pm 0.006 \times 10^5$ Pa, respectively. Another measurement of relative humidity is the dew point temperature, an important parameter for aviation. At the dew point temperature, water vapor will condense, also known as the saturation point. The dew point temperature is associated with the inlet temperature and relative humidity. Figure 2 shows how the tunnel stagnation dew point temperature varies with relative humidity level. A well-known approximation [14] used to calculate the dew point is

$$T_d = \frac{b\gamma(T, RH)}{a - \gamma(T, RH)} - 273 \tag{1}$$

where

$$\gamma(T, RH) = \frac{aT}{b + T} + \ell_n(RH)$$

and $a = 17.27$ and $b = 237.7$°C. The accuracy of the humidity was estimated to be $\pm 0.02$ for each experiment at the flow inlet shown in Fig. 2.

**Table 1 Characteristic parameters of the incoming boundary layer**

| $M_\infty$ | $\delta$ | $Tu$ | $H$ | $Re_\theta$ |
|---|---|---|---|---|
| 0.783 | 5.60 mm | 0.35% | 1.40 | 11,000 |
| 0.805 | 5.30 mm | 0.36% | 1.40 | 11,350 |

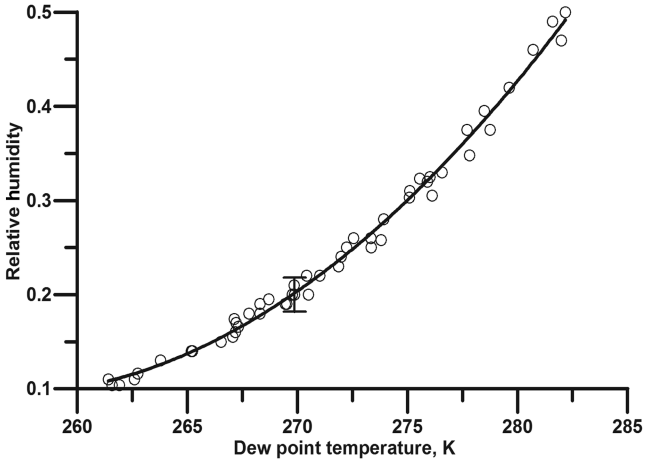


**Fig. 2 Relative humidity verses dew point temperature for the wind-tunnel inlet.**

## III. Results and Discussion

### A. Condensation Shock Wave

A series of tests were initially carried out at a tunnel freestream Mach number of 0.805 to identify condensation shock waves. Schlieren flow visualization illustrated the flow structures as the moist air flowed over the bump in the transonic wind tunnel, where the humidity levels were between 0.32 and 0.50.

As the flow passed over the bump, the drop in air pressure and temperature resulted in air saturation and water vapor being formed, appearing ahead of the main shock wave. In general, homogenous condensation takes place accompanied with latent heat release to the surrounding flow. The nonequilibrium process leads to changes in the thermodynamics and flow properties ahead of the main shock wave. As the humidity increases, fluctuations in the water vapor increase in the condensation process as well as pressure fluctuations causing the compression or condensation shock waves to form. Schnerr and Dohrmann [1] tested a circular arc model for humidity levels over 0.57. A double-shock system was observed where condensation shock waves appeared ahead of the main shock waves. Figures 3a–3c show that condensation shock waves appear upstream of the bump model highlighted by the dashed line. As humidity levels decreased, the λ-condensation shock wave was seen to meet the tunnel roof while the main shock waves were positioned further downstream, increasing in height.

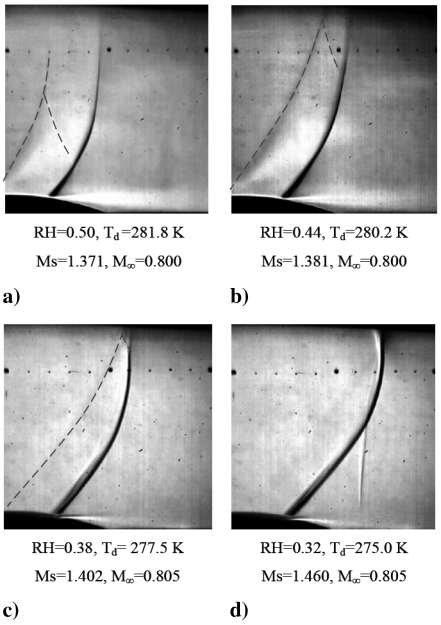


**Fig. 3 Schlieren images of shock waves over the bump model, $M_\infty = 0.800$–$0.805$.**

The static pressure measurements were taken coinciding with the relative humidity levels corresponding to Fig. 3. Mach numbers (Fig. 4) were obtained from the static pressures measured at the wall and from the inlet stagnation pressures, assuming the flow to be isentropic. However, it was shown [2] that, as the two shock waves (condensation and main) interacted with each other, the heat transfer from the condensation changed the flow properties as well as the pressure distribution. Hence, changes of pressure distribution in high humidity levels are expected to be a nonequilibrium process [4].

The humidity has little influence on the freestream velocity (the velocity variation is typically less than 1.2 m/s), but the Mach number profiles and separation lengths are clearly a function of humidity/dew point temperature. The results (Fig. 4) show how the relative humidity levels change the flow dynamics of the shock/boundary-layer interaction. In this case, the flow ahead of the main shock wave decelerated and caused the shock wave to move upstream.

### B. Humidity Effect on Shock Wave and Mach Number Distribution

The previous discussions have presented how condensation has an effect on shock/boundary-layer interactions. However, the previous results showed that the main shock wave interfered with the tunnel roof. To mimic a free-flight test, a shock wave free condition is needed. To achieve this, the freestream Mach number was reduced from 0.805 to 0.783.

Figures 5a–5f show shock wave positions on the bump in various humidity conditions for a tunnel freestream Mach number of 0.781, 0782, and 0.783. The condensation shock wave was only observed when the relative humidity was greater than 0.40 (Figs. 5a and 5b). The strength of the condensation shock wave in this series of tests were not as strong as in the case of $M_\infty = 0.805$, indicating that the condensation shock wave is also dependent on the Mach number upstream of shock wave. The compression waves observed in front of the shock waves are due to streamlines deflected over the bump in the supersonic region.

For humidity levels ranging from 0.30 to 0.25 (Figs. 5c and 5d), the condensation shock wave was not observed. This being said, the water vapor propagation downstream of the shock wave was observed during these tests (white dashed circle region). This same phenomenon was illustrated in Doerffer et al.'s schlieren flow visualization [6]. At humidity levels below 0.20 (Figs. 5e and 5f), a condensation shock wave or water vapor were barely visible, indicating that the condensation process was receding, resulting in the increase of the shock wave strength.

The Mach number distribution profiles are shown in Fig. 6 for the reduced freestream Mach number of 0.781–0.783. Increases in humidity levels resulted in decreased peak Mach numbers and the length of the separation region. The Mach number distribution and peak Mach number are sensitive to the humidity levels. At humidity levels below 0.15, the discrepancy between the Mach profiles becomes negligible. This result suggests that, if the humidity level is lower than 0.15, the effects become independent to the Mach number distribution.

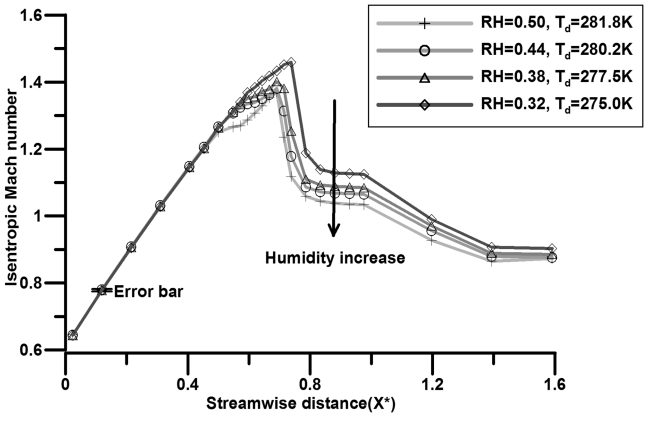


**Fig. 4 Mach number distribution over the bump, $M_\infty = 0.800$–$0.805$.**

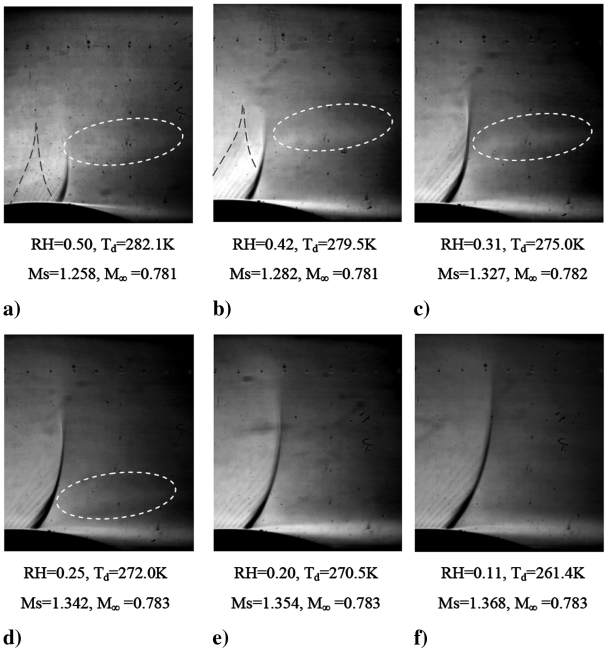


**Fig. 5 Schlieren images of shock waves over bump model, $M_\infty = 0.781–0.783$.**

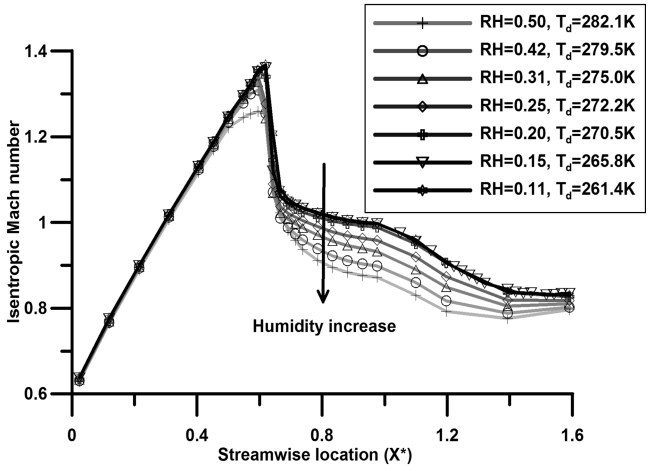


**Fig. 6 Mach number distribution over the bump, $M_\infty = 0.781–0.783$.**

### C. Humidity Effect on the Peak Mach Number

The effect of humidity on the peak Mach number normalized with the peak Mach number for the dry case is shown in Figs. 7a and 7b as a function of relative humidity and dew point temperature, respectively. Doerffer et al.'s experimental results [6] are also plotted. A general trend of decreasing peak Mach numbers at higher humidity levels was found in both experiments. It is also shown that, depending on the freestream Mach number, there is a large variability in the peak Mach number, where higher Mach numbers upstream of shock results in greater peak Mach number reductions. For the case of $M_\infty = 0.783$, increases in humidity levels from 0.15 to 0.50 resulted in the peak Mach number decreasing by up to 8%.

The humidity influence on the peak Mach number can be divided into three regions. When the humidity level is below 0.15, or a dew point temperature of 268 K, peak Mach number was relatively constant. As a result, it can be inferred that the air is dry. At humidity levels between 0.15 and 0.25, or dew point temperatures between 268 and 274 K, water vapor propagation downstream is barely visible and the relationship between the peak Mach number and humidity somewhat linear. Above humidity levels of 0.25, or a dew point temperature of 274 K, the condensation process highly affects the main shock wave and results in a nonlinear decrease in the peak Mach number.

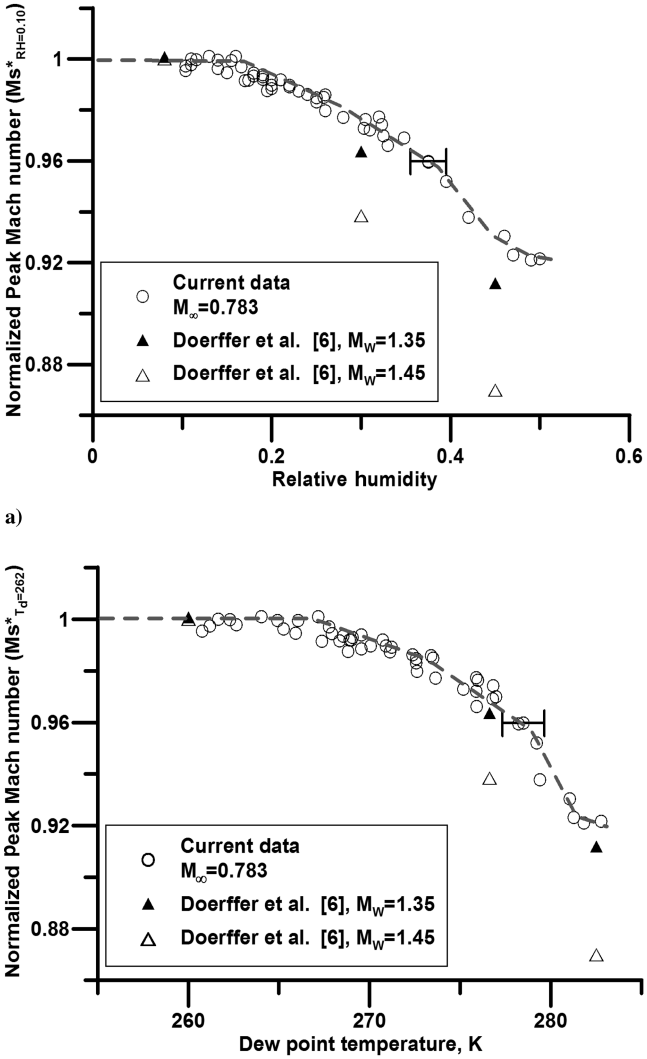


**Fig. 7 Normalized peak Mach number as a function of a) relative humidity and b) dew point temperature.**

### D. Humidity Effect on Shock Wave Position

The shock wave shift was estimated by comparing the position of the peak Mach number in a dry case normalized with the maximum shift. Shock wave shift was also calculated by Schnerr and Dohrmann [1] and Rusak and Lee [4], and are also illustrated in Fig. 8. The numerical results showed that a maximum shock wave forward shift appeared at a humidity level of 0.50. The experimental results presented in this work showed this shift to be at a humidity

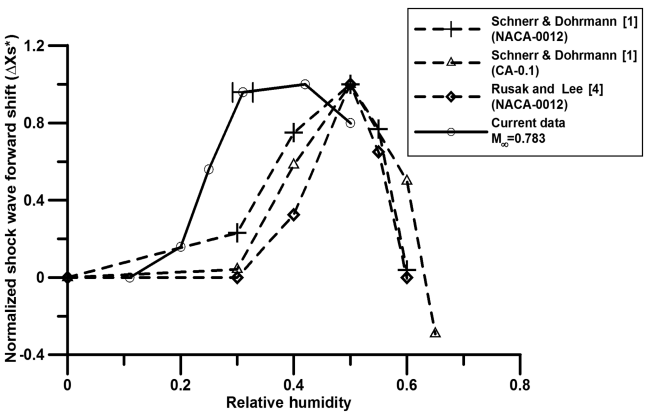


**Fig. 8 Main forward shock wave shift as a function of relative humidity.**

level of around 0.40. Upstream shock wave shift is due to the condensation process taking place and results in heat addition retarding the flow. Once the heat supply from condensation is more than the flow can absorb, that is, flow is in a high-humidity environment, a weak condensation shock wave appears. This results in increases in pressure and temperature behind the condensation shock wave, pushing the main shock wave downstream. This explains why the maximum forward shift appears up until the condensation shock wave appears.

### E. Humidity Effect on the Shock Wave Strength

The effect of humidity on shock wave strength, in terms of the pressure rise across the shock normalized to that of a dry air condition (air humidity of 0.10 or dew point temperature of 262 K), is shown in Fig. 9. The normalized shock strength form is given in Eq. (2) as

$$\Delta P_s^* = \frac{P_2 - P_1}{(P_2 - P_1)_{RH=0.10}} \tag{2}$$

where subscripts 1 and 2 indicate the pressure before and after the shock wave, respectively.

The change in shock wave strength as a function of humidity and dew point temperature is shown in Figs. 9a and 9b, respectively, along with the numerical and experimental results from Schnerr and Dohrmann [1], Rusak and Lee [4], and Doerffer et al. [6]. The shock wave strength starts decreasing when the humidity level is over 0.15, as shown in Fig. 9a. The discrepancy between the experimental and numerical results may be due to the inviscid method used. The correlation between stagnation dew point temperature and shock strength are shown in Fig. 9b. At stagnation dew point temperatures below 268 K, the shock wave strength remains unchanged, where the humidity effects are negligible. The shock wave strength can therefore be presented as a function of relative humidity or dew point temperature. The least-rms-error method was used to fit the current experimental data. The empirical correlations between shock wave strength and the humidity level or dew point temperature are given in Eqs. (3) and (4), respectively, as

$$\Delta P^*_{sRH=0.10} = \frac{1}{1 + (RH/0.567)^{3.70}} \tag{3}$$

$$\Delta P^*_{sT_d=262} = \frac{1}{1 + (T_d/284.5)^{70}} \tag{4}$$

From the best fit, Eqs. (3) and (4), it can be determined that when the stagnation humidity level reaches 0.31, or a dew point temperature of 275.0 K, the pressure drop is typically only 10% of that obtained in the dry air test, indicating that 10% of the shock wave strength was measured.

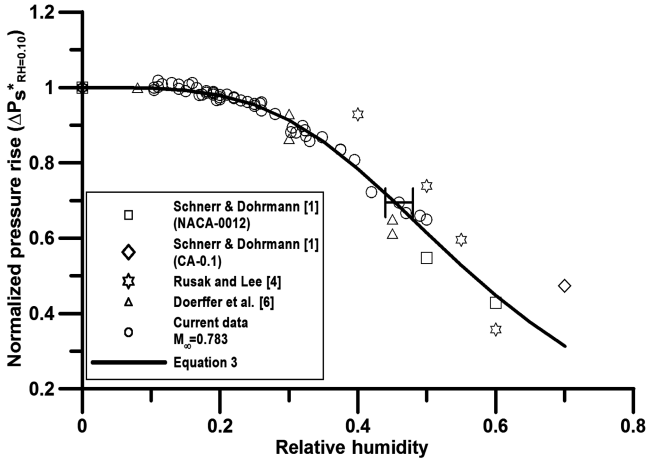


a)

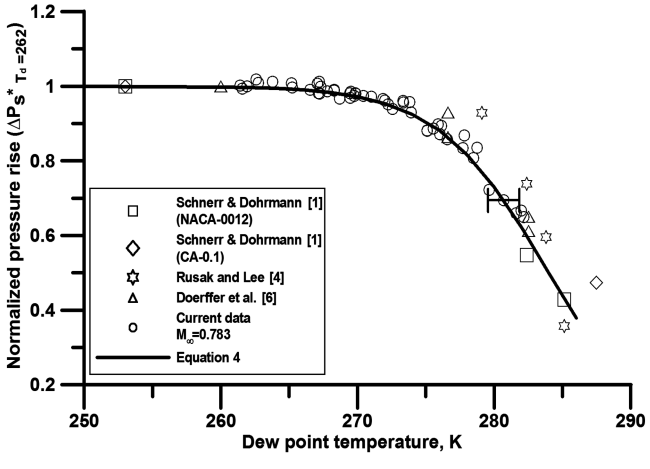


b)

**Fig. 9 Shock wave strength as a function of a) relative humidity and b) dew point temperature.**

### F. Humidity Effect on Shock-Induced Separation

The Mach number profiles over the wall-mounted bump (Fig. 6) showed that separation lengths were shorter for higher humidity levels. The humidity effects over the separation length can be investigated by means of china clay flow visualization. The results from the china clay flow visualization showed that the separation length is highly influenced by the condensation process in the wind tunnel (Fig. 10). The separation length was normalized with the dry air test and reduced to 75% at a dew point temperature of 277 K. A reduction of separation length in the humid air was also reported by Doerffer et al. [6], who used oil flow visualization. In Doerffer et al.'s experiments, the Mach number was fixed while the humidity levels were varied. This explains why the reduction ratio in separation length is different between Doerffer et al.'s experiments and the current results.

An example of correlation between shock wave strength and separation length is shown in Fig. 11 of the data corresponding to Fig. 10. The air humidity weakens the mechanism of shock wave boundary-layer interaction, and results in a reduction of the shock wave strength and a shorter separation length. Pearcy [15] showed that, if the pressure ratio rise across the shock wave is less than 1.40, there is no separation occurring at the foot of the shock wave. The results suggested that the humidity can weaken the shock wave strength, resulting in a shorter separation length.

### G. Comparison at the Same Shock Wave Position

To have the identical shock wave position for the humid and dry case, the outlet pressure was adjusted. These two flow cases are

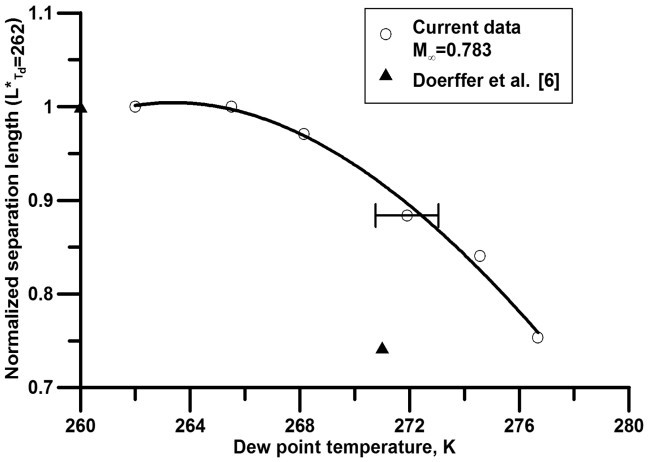


**Fig. 10 Shock-induced separation length as a function of dew point temperature.**

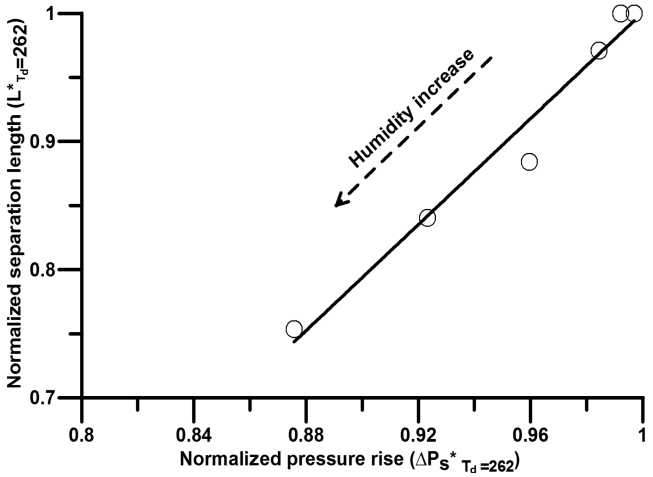


**Fig. 11 Shock-induced separation length as a function of pressure rise.**

compared to show the effect of humidity for the same shock wave position, and Fig. 12 shows the isentropic Mach number distribution at humidity levels of 0.50 and 0.10. The peak Mach number in the dry case is much stronger than in the humid case and results in a stronger separation. A longer separation length was found in the dry case. Similar results were found in Doerffer and Szumowski's Reynolds-averaged Navier–Stokes computation [7].

### H. Humidity Effect on the Shock Wave Strength Alone

To investigate the humidity effect only on the main shock wave, an identical shock wave strength was fixed (height of $32 \pm 1$ mm) in the dry and humid cases by adjusting the freestream Mach number. The Mach number distributions (Fig. 13) in two extreme cases of humidity, 0.11 and 0.50, showed that the condensation shock wave has an influence on the supersonic region around the shock wave. The condensation shock wave appears to delay the onset of the main shock wave. Little changes were found in the separation length. Wegener and Mack [5] conducted homogeneous condensation experiments in supersonic flow and showed that the homogeneous process takes place along a relatively short distance, and could be a few percent of the aerofoil chord length. The current results support Wegener and Mack's finding and show how the condensation effect on the shock wave is local, mainly around the supersonic region. Similar tests were performed in an inviscid fluid flow simulation by Rusak and Lee [4], where the pressure coefficient distribution indicated a similar trend in the shock wave position delay.

### I. Humidity Effect on the Pressure Fluctuations

Matsuo et al. [9] conducted numerical experiments on a nonequilibrium condensation in a Laval nozzle and stated that, if the

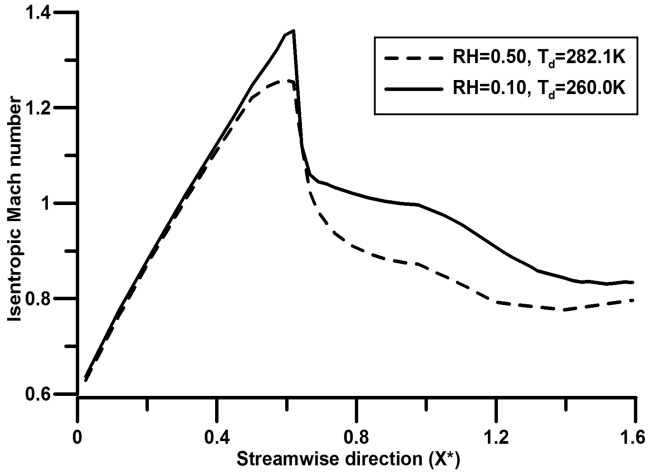


**Fig. 12 Mach number distribution in dry and humid conditions for the same shock wave position.**

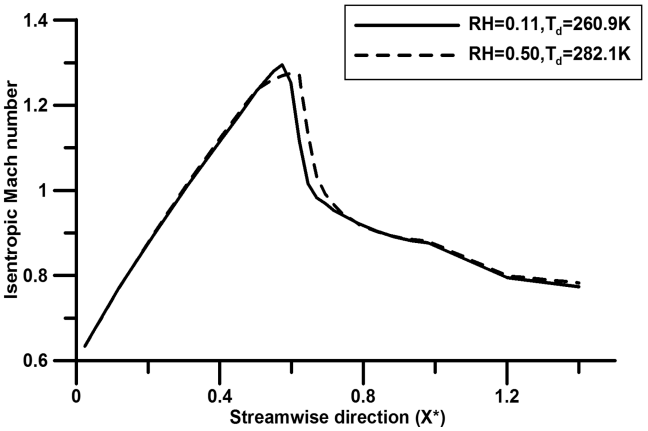


**Fig. 13 Mach number distribution in dry and humid conditions for an identical shock wave strength.**

latent heat released by condensation exceeds a certain quantity, the flow becomes unstable and a periodic flow oscillation occurs. The same conclusion was made by Rusak and Lee [4] using a small-disturbance model to calculate condensation effects in the transonic flow. The present study is to investigate the flow unsteadiness induced by a condensation shock wave.

Pressure fluctuations were measured across the shock wave and normalized with the freestream dynamic pressure $q$. The measurements were made at locations $X^* = 0.60$, 0.63, and 0.66, corresponding to the stations before, adjacent, and after the shock wave, respectively. Normalized pressure fluctuation is also a measurement of shock wave strength, and so Eqs. (3) and (4) for determining shock wave strength can be applied here. The functions of $P_{\text{rms}}/q$ in various humidity levels or dew point temperatures are given as

$$\left(\frac{P_{\text{rms}}}{q}\right)^*_{RH=0.10} = \frac{1}{1 + (RH/0.567)^{3.70}} \tag{5}$$

$$\left(\frac{P_{\text{rms}}}{q}\right)^*_{T_d=262} = \frac{1}{1 + (T_d/284.5)^{70}} \tag{6}$$

Equation (6) is shown in Fig. 14 together with experimental measurements and shows a very good correlation. The empirical function can be used to determine shock wave strength at various flow humidity levels. At the location of $X^* = 0.60$, the maximum value was found at a dew point temperature of 276 K (humidity level of 0.35). This is due to the shock wave shifting forward. The forward shift indicates a high-pressure fluctuation of the shock wave approaching station 1 ($X^* = 0.60$). Once the shock wave shifted backward, the pressure fluctuations decreased at station 1, while

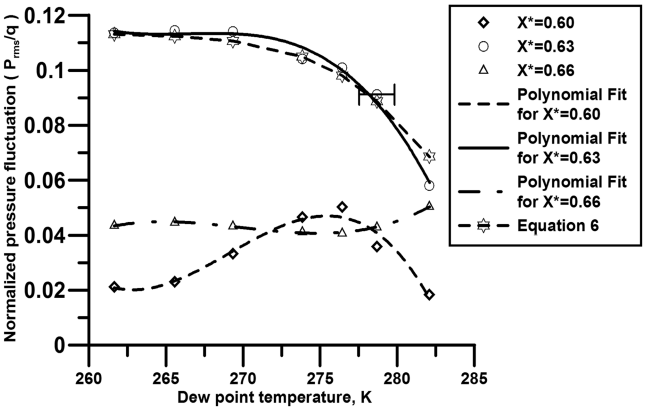


**Fig. 14 Pressure fluctuations across shock wave as a function of dew point temperature.**

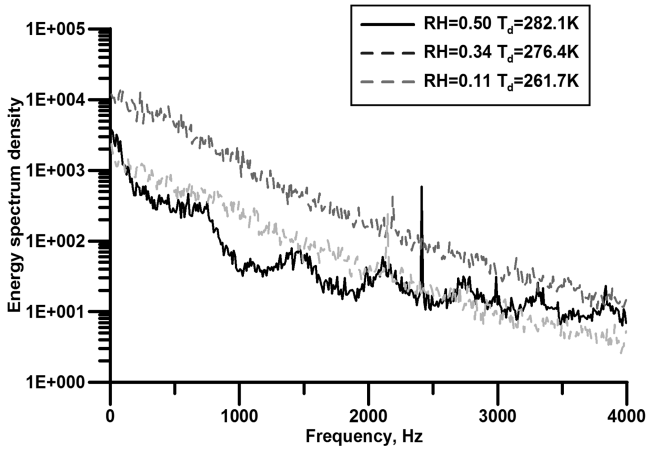


a)

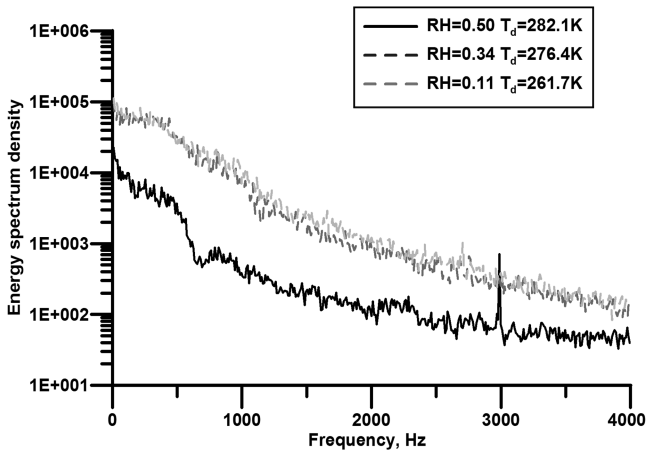


b)

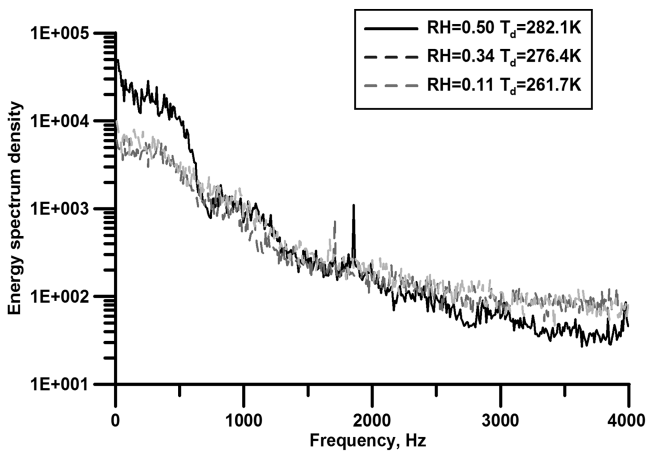


c)

**Fig. 15 Pressure fluctuation spectrum in the humid and dry tests: a) $X^* = 0.60$, b) $X^* = 0.63$ (adjacent to the shock wave position), and c) $X^* = 0.66$.**

increasing at station 3 ($X^* = 0.66$). Pressure fluctuations remained almost constant at a dew point temperature below 266 K, where the shock wave dynamics are independent of the humidity effects.

In a high-moisture test condition, the relative humidity can reach 0.50 (similar to Fig. 5a). The λ-condensation shock wave appears ahead of the main shock, superimposed on the foot of the main shock wave at location $X^* = 0.60$. A fast Fourier transform was used to locate the unsteady periodic frequencies. Comparison between three different humidity level test cases were presented in Figs. 15a–15c, at three different streamwise locations. The onset of unsteadiness was found at approximately 720 Hz and was shown to be harmonically periodic at this frequency for a humidity level of 0.50. No unsteadiness was found in the dry cases. This corresponds to Matsuo et al.'s [9] conclusion that the condensation process will result in unstable periodic flow oscillations only when the humidity level exceeds 0.50. In the relative humidity case of 0.50, the shock wave strength is weakened by the condensation, and therefore the pressure fluctuation energy level is generally lower than a dry case. When the humidity levels decrease, the condensation shock wave moves toward the tunnel roof and the high-frequency condensation shock-induced unsteadiness was difficult to measure from the surface-mounted Kulite. The unsteadiness was also measured at the interaction region between the two shock waves and demonstrates that the unsteadiness is very local and does not propagate over long distances.

## IV. Conclusions

The humidity effects on the shock/boundary-layer interaction in a transonic flow have been investigated through the steady and unsteady measurements at humidity levels ranging from 0.10 to 0.50, where the corresponding dew point temperature is between 260 and 285 K.

1) There are significant effects of humidity on shock/boundary-layer interaction. At high-humidity levels (above 0.40), condensation shock waves may appear in a λ shape, ahead of the main shock wave.

2) The humidity effects on the shock wave strength can be represented by an empirical function of $\Delta P_s^*$ and relative humidity or dew point temperature.

3) For humidity levels below 0.15, or a dew point temperature of 268, both the peak Mach number and Mach number distribution become independent of the humidity. Therefore, tests with humidity levels below 0.15 can be regarded as dry air cases.

4) For a given freestream Mach number, the humidity influence is only local to the supersonic region around the shock wave. The Mach number profile in the separation region has no significant change.

5) The condensation shock wave leads to a self-excited unsteady flow, and a periodic harmonic unsteady frequency of 720 Hz was measured at the interaction between two shock waves. The unsteadiness resulting from the condensation has a local influence on the main shock wave.

6) The unsteady pressures can be represented by an empirical function of $P_{\text{rms}}/q^*$ and relative humidity or dew point temperature.

## Acknowledgments

The work presented in this paper is carried out within the framework of the EU-FP6 Unsteady Effects of Shock Wave Induced Separation Research Program and is financially supported by the European Commission (EC FP6 AST-CT-2005-012226 UFAST). The authors would also like to thank P. Doerffer for his constant support and advice.

## References

[1] Schnerr, G. H., and Dohrmann, U., "Transonic Flow Around Airfoils with Relaxation and Energy Supply by Homogeneous Condensation," *AIAA Journal*, Vol. 28, No. 7, 1990, pp. 1187–1193. doi:10.2514/3.25190

[2] Schnerr, G. H., and Dohrmann, U., "Drag and Lift in Nonadiabatic Transonic Flow," *AIAA Journal*,Vol. 32, No. 1, 1994, pp. 101–107. doi:10.2514/3.11956

[3] Campbell, J. F., Chambers, J. R., and Rumsey, C. L., "Observation of Airplane Flow Fields By Natural Condensation," *Journal of Aircraft*, Vol. 26, No. 7, 1989, pp. 593–604. doi:10.2514/3.45809

[4] Rusak, Z., and Lee, J. C., "Transonic Flow of Moist Air Around a Thin Airfoil with Non-Equilibrium and Homogeneous Condensation," *Journal of Fluid Mechanics*, Vol. 403, 2000, pp. 173–199. doi:10.1017/S0022112099007053

[5] Wegener, P. P., and Mack, L. M., "Condensation in Supersonic and Hypersonic Wind-Tunnels," *Advances in Applied Mechanics*, Vol. 5, 1958, pp. 307–447.

[6] Doerffer, P., Szumowski, A., and Yu, S., "The Effect of Air Humidity on Shock Wave Induced Incipient Separation," *Journal of Thermal Science*, Vol. 9, No. 1, 2000, pp. 45–50. doi:10.1007/s11630-000-0044-8

[7] Doerffer, P., and Szumowski, A., "Numerical Analysis of Shock Induced Separation Delay by Air Humidity," *Journal of Thermal Science*, Vol. 14, No. 2, 2005, pp. 120–125. doi:10.1007/s11630-005-0021-3

[8] Evans, N. A., "Transonic Nozzle Flow Instabilities Due to Shock Wave/ Condensation Front Interaction," *AIAA 19th Fluid Dynamics, Plasma Dynamics and Lasers Conference*, AIAA Paper 87-1355, 1987.

[9] Matsuo, S., Kawagoe, S., Sonoda, K., and Setoguchi, T., "Oscillations of Laval Nozzle Flow with Condensation, Part 1: On the Range of Oscillations and Their Frequencies," *Bulletin of the JSME*, Vol. 26, No. 219, 1983, pp. 1556–1562.

[10] Matsuo, S., Tanaka, M., Setoguchi, T., and Kim, H. D., " Numerical Visualization of Moist Air Flow Through the Ludwieg Tube," *Proceedings of the 13th International Symposium on Transport Phenomena*, 2002, pp. 151–156.

[11] Setoguchi, T., Matsuo, S., Shimamoto, K., Yasugi, S., and Yu, S., "Passive Control of Unsteady Condensation Shock Wave," *Journal of Thermal Science*, Vol. 9, No. 4, 2000, pp. 299–304. doi:10.1007/s11630-000-0067-1

[12] Raghunathan, S., and McAdam, R. J. W., "Free-Stream Turbulence and Transonic Flow over a Bump Model," *AIAA Journal*, Vol. 21, No. 3, 1983, pp. 467–469. doi:10.2514/3.8096

[13] Raghunathan, S., "Passive Control of Shock-Wave Interaction," *Progress in Aerospace Sciences*, Vol. 25, No. 3, 1988, pp. 271–296. doi:10.1016/0376-0421(88)90002-4

[14] Riegel, C., *Fundamentals of Atmospheric Dynamics and Thermodynamics*, World Scientific, Singapore, 1989.

[15] Pearcy, H. H., "Some Effects of Shock-Induced Separation of Turbulent Boundary Layers in Transonic Flow Past Aerofoils," *Aeronautical Research Council Reports and Memoranda*, Aeronautical Research Council No. 3180, London, 1959.